DEVELOPMENTAL DYNAMICS 241:863–878, 2012

RESEARCH ARTICLE

Normalized Shape and Location of Perturbed Craniofacial Structures in the *Xenopus* Tadpole Reveal an Innate Ability to Achieve Correct Morphology

Laura N. Vandenberg, Dany S. Adams, and Michael Levin*

Background: Embryonic development can often adjust its morphogenetic processes to counteract external perturbation. The existence of self-monitoring responses during pattern formation is of considerable importance to the biomedicine of birth defects, but has not been quantitatively addressed. To understand the computational capabilities of biological tissues in a molecularly tractable model system, we induced craniofacial defects in *Xenopus* embryos, then tracked tadpoles with craniofacial deformities and used geometric morphometric techniques to characterize changes in the shape and position of the craniofacial structures. Results: Canonical variate analysis revealed that the shapes and relative positions of perturbed jaws and branchial arches were corrected during the first few months of tadpole development. Analysis of the relative movements of the anterior-most structures indicates that misplaced structures move along the anterior–posterior and left–right axes in ways that are significantly different from their normal movements. Conclusions: Our data suggest a model in which craniofacial structures use a measuring mechanism to assess and adjust their location relative to other local organs. Understanding the correction mechanisms at work in this system could lead to the better understanding of the adaptive decision-making capabilities of living tissues and suggest new approaches to correct birth defects in humans. *Developmental Dynamics 241:863–878, 2012.* © 2012 Wiley Periodicals, Inc.

Key words: geometric morphometrics; canonical variate analysis; principle components analysis; H^+-V-ATPase; neural crest; robustness

Key findings:

- Craniofacial perturbations in the *Xenopus* tadpole become normalized over time.
- The jaw and branchial arches achieve both normal position and morphology. Eyes, nose and otoliths achieve normal position but varying degrees of normal morphology.
- Two parameters, distance from the brain and angle from the midline, define normal position of craniofacial structures. Perturbed structures eventually achieve normal values for these parameters even though they start from abnormal initial conditions.
- These results shed light on the information processing and decision-making processes that underlie biological tissues' innate ability to repair deformities.

Accepted 27 February 2012

Center for Regenerative and Developmental Biology, and Biology Department, Tufts University, Medford, Massachusetts
Grant sponsor: NRSA; Grant number: 1F32-GM087107; Grant sponsor: NIH; Grant number: K22-DE016633; Grant sponsor: G. Harold and Leila Y. Mathers Charitable Foundation.
***Correspondence to: Michael Levin, 200 Boston Avenue, Suite 4600, Medford, MA 02155. E-mail: michael.levin@tufts.edu**

DOI 10.1002/dvdy.23770
Published online 23 March 2012 in Wiley Online Library (wileyonlinelibrary.com).

Developmental Dynamics

INTRODUCTION

A fundamental understanding of complex pattern formation (self-assembly of structures such as the eye, limb, or the entire bodyplan during embryogenesis or regeneration) requires more than pathway data on protein interactions and gene networks. It is also necessary to integrate those data into modular functions that explain higher-level topological properties such as anatomical polarity, size control, and symmetry. Achieving such understanding is a difficult task because large numbers of small, diverse building blocks (cells) must coordinate their individual activities to achieve geometric goals defined at the level of the whole system. At the same time, predictive control of biological systems composed of large numbers of heterogeneous active agents (cells in vivo) is a key goal of regenerative medicine.

Two approaches to understanding emergent behavior of large numbers of components have been highly successful outside of biology. In physics, "least action" principles describe a system's behavior in terms of maximizing (or minimizing) some well-defined quantity, such as entropy, energy, or symmetry. The resulting statistical mechanics deals with systems (e.g., gasses) as ensembles of lower-level units, giving rise to a mature science of thermodynamics and near-ubiquitously applicable concepts like entropy (Goodwin, 1964; Brooks and Wiley, 1988; Weber et al., 1988). In computer science, a system's behavior is described in terms of the data that a given information-processing algorithm uses to make decisions. In this approach, neither matter nor energy but information exchanged among black-box components is used as the perspective from which quantitative predictions of physical (Frieden, 1998; Siegfried, 2000) and social (Langton, 1995; Couzin, 2009; Deisboeck and Couzin, 2009) systems are derived.

Applying cybernetic paradigms to developmental biology requires that we formulate models of what quantities morphogenetic systems seek to maximize, and what information cells use to make decisions about their behavior. Unfortunately, there has been a dearth of quantitative data from which testable models of this type can be inferred. An especially fertile ground for developing novel approaches to large-scale patterning is the regulative nature of embryogenesis. It has long been known that in many species, developmental programs are not "hardcoded" (occurring in the same way regardless of circumstances) but in fact are able to correct for a large number of significant external perturbations. Thus they achieve the desired goal anatomy by initiating and modulating morphogenetic events that compensate for deviations from the normal progression of events by using a flexible, adaptive response to current state information. One example is the production of two complete (albeit smaller) animals when an early frog or mouse embryo is split in half. Another is the regeneration of a perfectly sized, placed, and oriented limb when a salamander's appendage is amputated in adulthood. A myriad of examples familiar to classical developmental and regenerative biologists show that patterning systems can detect damage (deviation from a predetermined target morphology), take steps to correct their pattern toward that goal state, and stop growth or rearrangements at the correct time. Indeed, this sometimes uses un-natural intermediate stages (Voskoboynik et al., 2007). For our understanding of these processes to aid in design of biomedical strategies, quantitative analysis of morphological responses to perturbations must nucleate predictive models of tissue behavior. We sought to establish a proof of principle approach using quantification of shape and shape changes during experimentally altered development in a genetically tractable model system, to derive hypotheses about what information tissues have and exchange, and what actions lead to normalization during complex pattern formation.

Congenital malformations of craniofacial structures comprise a significant class of birth defects with serious repercussions for affected individuals. Some conditions including cleft lip, cleft palate and micropthalmia affect more than 1 in every 600 births (Dolk et al., 2010). Both genetic and environmental factors contribute to these types of birth defects (Sant'Anna and Tosello, 2006; Hart and Hart, 2009; Brugmann et al., 2010) and many cannot be repaired with surgery (Saadeh et al., 2008). Fetal mice with mutations affecting craniofacial development have been successfully treated with pharmaceuticals that specifically modify expression of target genes implicated in craniofacial defects (Jones et al., 2008), suggesting that some patterning defects can be abrogated in the womb by targeted modulation of patterning processes. Such interventions require detailed understanding of the mechanisms that establish and maintain complex pattern in the embryonic face.

In vertebrates, cranial neural crest (CNC) cells contribute to the bones of the jaw, the teeth, and craniofacial cartilage. In frog embryos, a population of CNC cells migrates collectively out from the border of the neural plate, before neural tube closure, to form these craniofacial structures (Sadaghiani and Thiebaud, 1987; Mayor and Aybar, 2001). The signals necessary for the induction, specification, migration, and differentiation of these cells into the structures of the head and face have been well characterized (Basch et al., 2004; Alfandari et al., 2010; Theveneau and Mayor, 2011). Other structures of the face including the eye lens, olfactory bulb, and otic vesicle develop from cranial placodes—specialized regions of the ectoderm (Brugmann and Moody, 2005; Streit, 2007). The placodes originally form as thickened areas of the ectoderm that invaginate to produce the sensory organs. While neural crest and placodes develop in similar ways from similar cell populations, the placodes have a more restricted developmental potential and are significantly less migratory (Schlosser, 2006).

Although our descriptive knowledge of the normal embryonic differentiation of craniofacial structures is quite good, quantitative understanding of their remodeling under perturbation is largely lacking (Zambuzzi et al., 2009; Parsons et al., 2011). What deviations from the normal course of development can be sensed by this system, and what information do cells use in the repair process? One

extremely powerful tool for analyzing craniofacial morphologies is geometric morphometrics of 2-dimensional and 3-dimensional images and structures (Singh, 2008). Geometric morphometric analysis involves the identification of landmarks on samples that mark discrete anatomical features; the alignment of landmarks using a mathematical algorithm that removes information about scale and rotation of specimens; and the use of multivariate statistics to study relationships among groups of samples (von Cramon-Taubadel et al., 2007). This analytical method has been applied to the study of craniofacial structures across human populations (Weisensee and Jantz, 2011), as a means to determine the effectiveness of treatments for craniofacial malformations (Singh et al., 2005), to diagnose craniofacial anomalies (Harris and Ross, 2008), to classify the effects of craniofacial toxicants (Klingenberg et al., 2010), to characterize long-range signaling in appendage regeneration (Mondia et al., 2011), and even to determine the age at which the human skull reaches fully formed adult features (Ross and Williams, 2010). Similar studies have also been performed on craniofacial structures of fish (Cooper et al., 2010; Suzuki et al., 2010; Parsons et al., 2011).

To better understand the self-regulating capabilities of craniofacial patterning mechanisms, we perturbed the instructive signals provided by the endogenous electrical activity of the ion pump H^+-V-ATPase during *Xenopus* tadpole development. Loss of H^+-V-ATPase function leads to severe abnormalities in the jaws, branchial arches, eyes, otic capsules, and olfactory pits (Vandenberg et al., 2011). We raised and imaged tadpoles with craniofacial abnormalities over the course of several months and through metamorphosis. To track these abnormal tissues over this period of time, we used geometric morphometric analytical techniques to quantify and compare the relative morphologies of dorsal and ventral landmarks as tadpoles aged. We observed that abnormal jaws and branchial arches correct themselves over time. Other tissues such as the eye and nose achieve a more normal location, but have variable abilities to achieve a completely normal appearance. Remarkably, analysis of the data suggests that the individual structures of the face can sense their relative position and initiate the compensatory migration and/or remodeling that allows them to achieve a more normal location and morphology.

RESULTS

Perturbed Tadpole Faces Correct Their Anatomy Over Time

The first step to establish a model for analysis of shape robustness, self-monitoring, and repair of a complex multi-tissue organ system, is to quantify shape and shape change in such a system. We induced perturbations of the face of the *Xenopus* tadpole by injecting mRNA into only one cell at the two cell stage of development, thus generating tadpoles that have abnormal structures induced on only one side. Injection of mRNA encoding a dominant mutant form of ductin, subunit c of the H^+-V-ATPase, produces tadpoles with perturbed development of the eyes, jaws, branchial arches, nose, and otolith/otocyst (Vandenberg et al., 2011), but no systematic description of the patterning consequences of such changes has yet been attempted. To that end, we imaged affected tadpoles at several discrete periods after fertilization. Strikingly, as these tadpoles aged, the craniofacial perturbations (whether on the left, right, or both sides of the face) became less apparent over time, and relatively normal faces were constructed despite the deviations in initial states (Fig. 1).

The structures that appeared to achieve the most normal appearance over time were the branchial arches and the jaw, which both move and remodel to achieve a more normal appearance as the tadpole ages. Additional craniofacial structures including the eyes, olfactory pits (nostrils) and otolith/otocysts, were able to regain a more normal position, although these tissues never achieved a completely normalized morphology (Fig. 2). The effects on the eyes were most pronounced, with abnormal shapes rarely changing, even over months (Fig. 2A). Affected nostrils, including those originally formed connected to the eye, did achieve a more normalize placement, but their morphology remained somewhat abnormal with strands of ectopic tissue between the nose and eye (Fig. 2A). Tadpoles that were missing otoliths in their otocyst cavities never produced these absent structures (Fig. 2B), and ectopic structures were never resorbed into the tadpole (Fig. 2B). We conclude that the process of development is not hard-coded but is able to achieve morphological goal states adaptively, altering at least some multi-cellular structures' behavior to compensate for significant experimentally-induced malformations.

Morphometric Analysis Reveals a Convergence of Shape in Later Stage Tadpoles

Using the MorphoJ geometric morphometrics program, we analyzed the shape changes of various craniofacial structures on the dorsal and ventral sides of tadpoles at various ages. To quantify changes in the relative position of craniofacial structures at various ages in unaffected and affected tadpoles, we identified 12 landmarks on the dorsal side of imaged tadpoles and 20 landmarks on the ventral side (Fig. 3). Descriptions of these landmarks are included in the Methods section. The position of these landmarks, and the relative variance of the positions within treatment groups, reveal how perturbations to the left or right side of the face influence the position of each structure of interest.

To determine whether the relative positions of each landmark and shapes of each structure of interest were affected at each age, principal components analysis (PCA) was performed separately within each group (unaffected, perturbed left side, perturbed right side) at each age. As these animals age, the overall size of their heads increases (length: 1.8 to 10 mm, width 3 to 8.5 mm). However, because this morphometric analysis is shape-based, it is not affected by size/scaling. Thus, changes are reported as "relative" positions because all

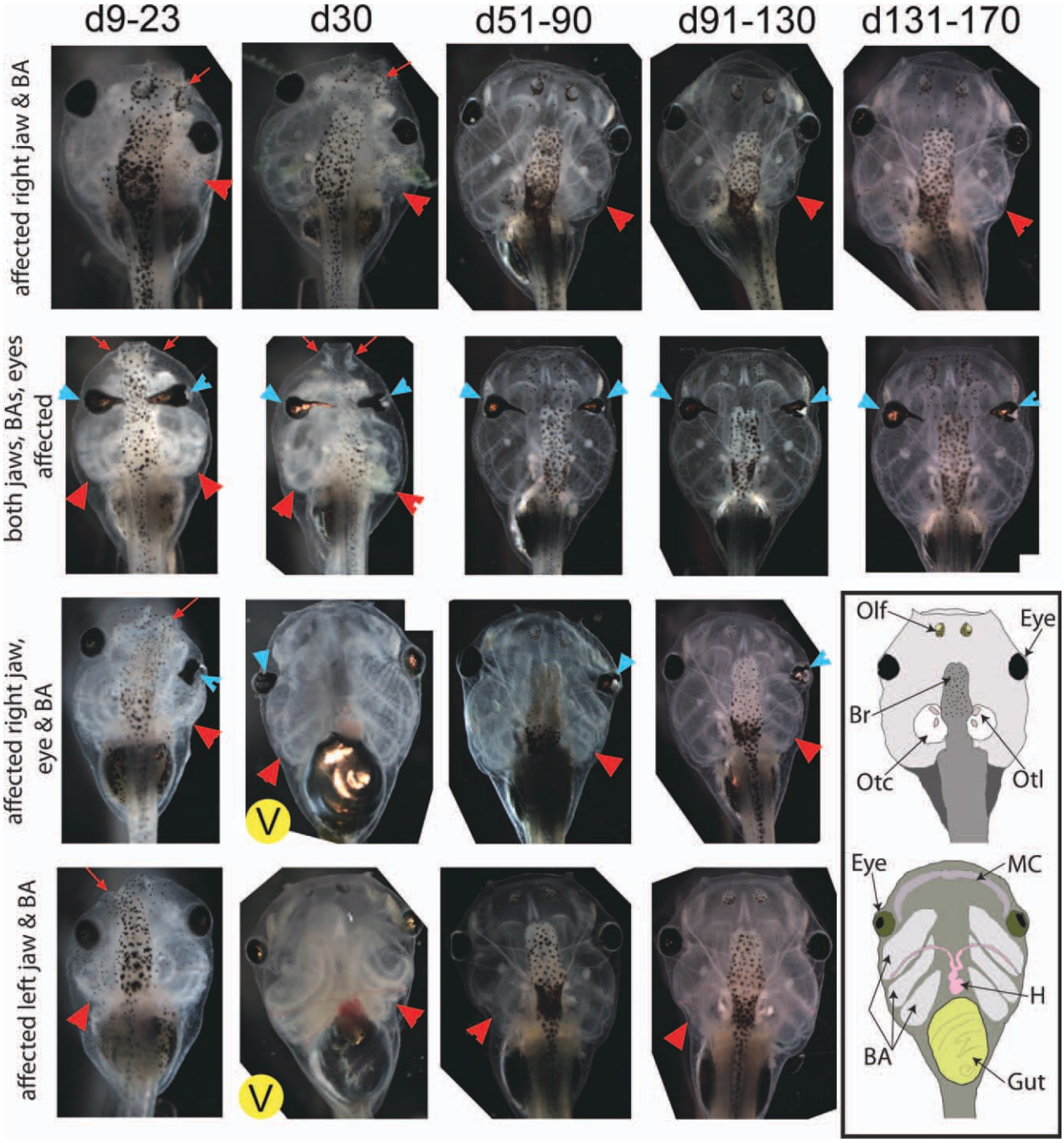

Fig. 1. Four examples of tadpoles with perturbed craniofacial structures. In all four examples, the malformed jaw and branchial arch structures appear to "normalize" over time. In contrast, eyes change somewhat in shape but are never completely normalized. In all panels, blue arrowheads indicate malformed eyes, red arrowheads indicate malformed branchial arches, and red arrows indicate malformed jaws. All images are dorsal views except two panels showing ventral views marked with a V. Inset: schematics of the dorsal (top) and ventral (bottom) structures of the head and face. Olf, olfactory bulbs (nostrils); Br, brain; Otc, otocyst; Otl, otolith; MC, Meckel's cartilage (mandible/jaw); H, heart; BA, branchial arches.

size-based differences are removed mathematically (Kendall, 1977). PCA is often the first morphometric analysis performed because it generates descriptive information about average shape changes within a group, while also reducing the number of variables without any major loss of information. The results of the PCA for each treatment and age were then superimposed onto an outline of the major craniofacial landmarks, to facilitate the visualization of the "average" effect of treatment on landmark position. In unaffected tadpoles, the most obvious change to the dorsal side was the elongation of the face as the animal aged (Fig. 4A). An increase in the relative size of the otocysts was also visible. In contrast, tadpoles with perturbed craniofacial structures show

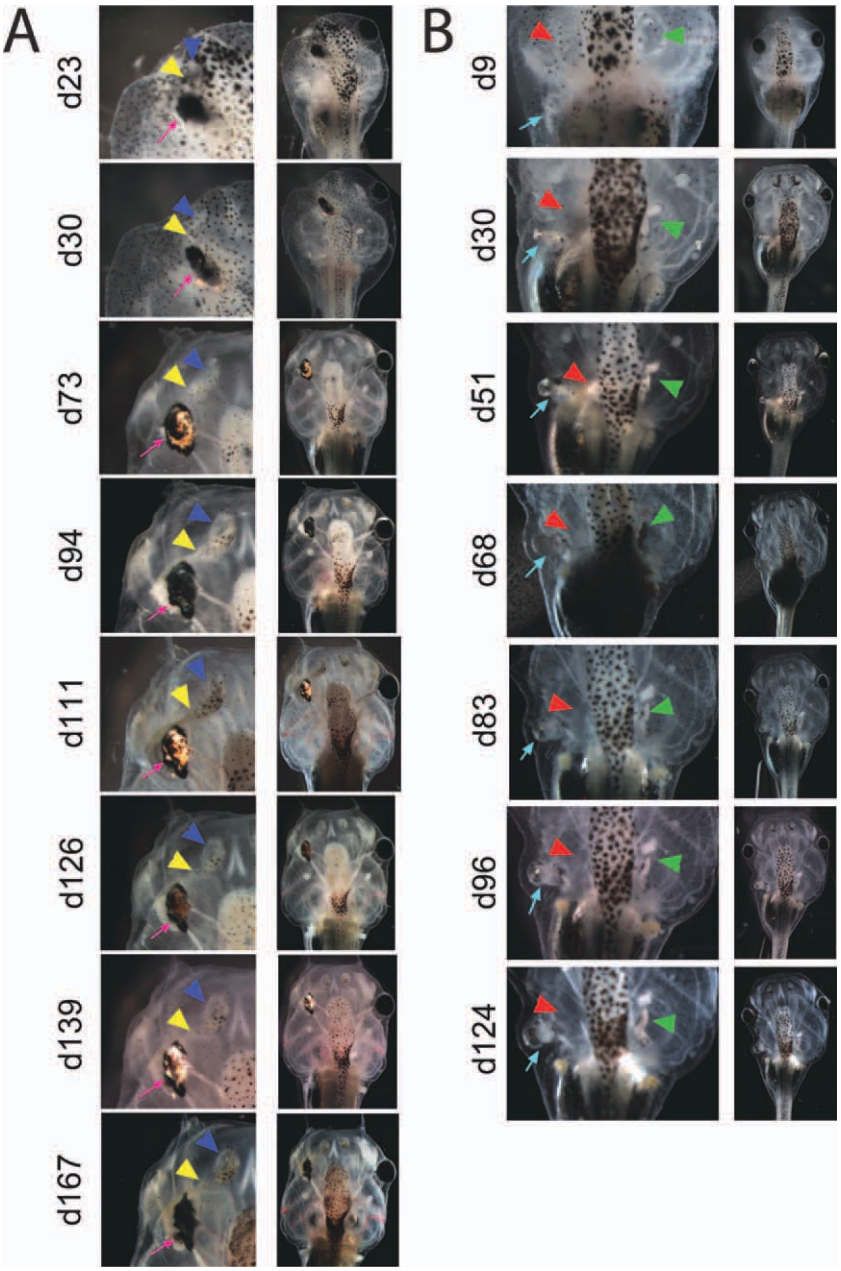

Fig. 2. Abnormalities in placode-derived tissues persist throughout tadpole stages. Placode-derived structures including eyes, nose, and otolith/otocyst were imaged in tadpoles over a range of ages. **A**: In a tadpole with conjoined eye–nose tissue at d9, a stalk of tissue clearly connects these two malformed structures. As the animal ages, the nostril moves away from the eye to its normal position, but a small strand of tissue remains connecting these structures. The eye is severely malformed at all ages examined. Pink arrow indicates eye, blue arrowhead indicates nostril, and yellow arrowhead points to the ectopic tissue connecting these two structures. **B**: A tadpole with a malformed left side is shown. The left otocyst is missing the otolith stones at all ages. Additionally, there is a pocket of abnormal ectopic tissue that is never resorbed. Green arrowheads indicate a normal otolith/otocyst, red arrowheads indicate an otocyst that is missing its otoliths, and the blue arrow indicates ectopic abnormal tissue.

deviations from the normal appearance of landmarks (Fig. 4A). At early ages (d9, d23, d30), analysis of dorsal images reveal that the eye on the perturbed side is typically positioned to the interior of the head, and the otoliths are normally positioned to an outer extreme. But at later ages (d51–90, d91–130, d131–167), the average location of these landmarks is more similar to what is observed in unaffected tadpoles.

PCA was also used to describe the ventral structures in all treatment groups. Elongation of the entire face occurred on the ventral side of unaffected tadpoles (Fig. 4B). Analysis of ventral PCA outlines collected from individuals with craniofacial perturbations revealed that the average affected individual had a noticeably smaller branchial arch on the affected side at early ages and an eye that bulged inward on that side (Fig. 4B). However, the outlines were visibly more normal at later ages. PCAs of landmarks on the dorsal and ventral sides of unaffected and unilaterally perturbed tadpoles support our visual observations that tadpoles with craniofacial abnormalities acquire a more normal appearance over time.

PCA allowed us to produce a statistical consensus of the observations within each treatment group and age. However, this analysis does not allow any statistical conclusions to be made *between* groups. To determine whether these three groups (unaffected, perturbed left side, perturbed right side) were statistically distinguishable from each other at different ages, we next performed canonical variate analysis (CVA). CVA includes a step to equalize the variance among groups, and thus allows for statistical comparisons of group shapes that are not possible with PCA alone. CVA revealed that the placement of ventral landmarks in these groups was significantly different at early ages (d9, d23, d30), but these differences were no longer apparent at later ages (d91–130, d131–167; Fig. 5A), confirming the remodeling capabilities of the face. Importantly, normalization that was observed at d90–130 occurred before the onset of hind-leg emergence, suggesting that these effects were not simply due to commenced metamorphosis (data not shown).

The analysis of dorsal landmarks revealed a more complex picture. At early stages (d9, d23), these three groups are statistically distinguishable (Fig. 5B). In contrast, images collected in the periods between d51–90 and d91–130 reveal few differences between the groups. But at the oldest stages examined (d131–167), the groups were once again statistically

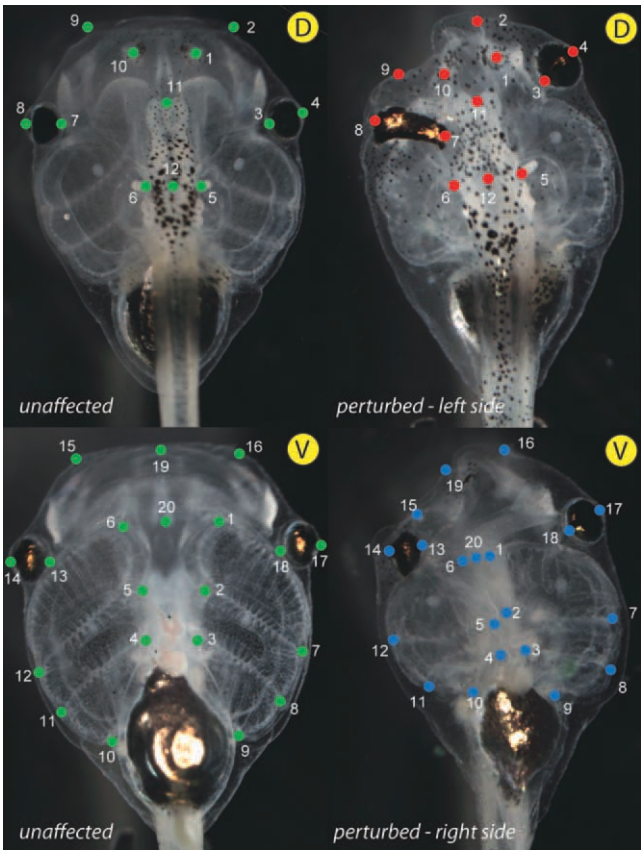

Fig. 3.

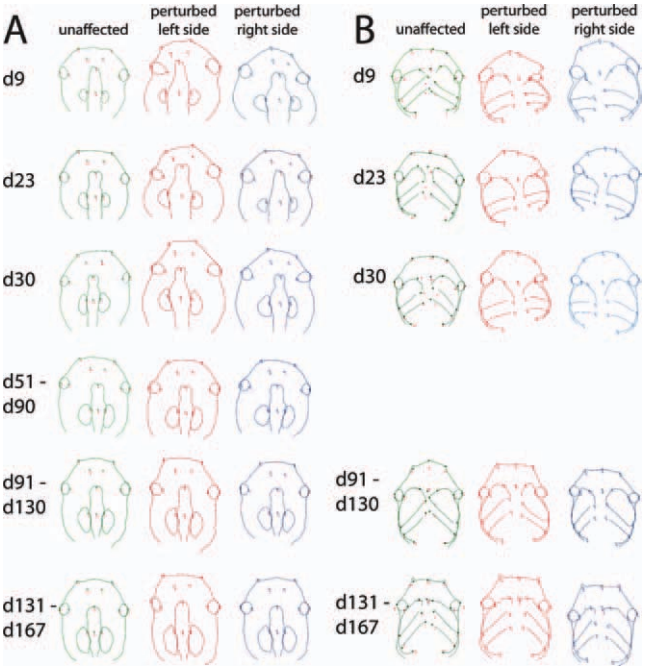

Fig. 4.

distinguishable. From these results we conclude that the dorsal landmarks—largely marking the location of sensory organs—respond to the normal developmental process differently than ventral landmarks (mostly representing the jaw and branchial arches). Furthermore, these results suggest that jaw and branchial arches in perturbed tadpoles are "normalized" to the point that they cannot be mathematically distinguished from unaffected tadpoles, but other dorsal structures like the eye are distinguishable even at late stages.

Correct Placement of Craniofacial Structures Is Driven by Dynamic Information, Not Predetermined Movements

We originally hypothesized that defects could be repaired on one side of the face by signals or information

Fig. 3. Dorsal and ventral landmarks used for morphometric analysis. A total of 20 ventral (V) and 12 dorsal (D) landmarks were selected on the images collected of unaffected and perturbed tadpoles at several ages. Only perturbed tadpoles with an affected left or right side were used for morphometric analysis; tadpoles with visible defects on both sides were not included. This figure shows the dorsal and ventral landmarks on unaffected and perturbed tadpoles at 23 days postfertilization (d23). Green, unaffected; red, perturbed on left side; blue, perturbed on right side.

Fig. 4. Outlines from principal components analysis (PCA) -derived landmark locations indicate that the average face appears to be normalized. **A**: PCA of dorsal landmarks for each treatment group and age reveal differences in the centroid placement for many landmarks at early stages. However, by later stages, the outlines derived from animals with craniofacial perturbations largely resemble the outlines derived from unaffected tadpoles. Green, unaffected; red, perturbed on the left side; blue, perturbed on the right side. **B**: PCA of ventral landmarks reveal centroid placements that do not appear to change considerably over time in unaffected tadpoles (green), with the exception of a lengthening of the anterior part of the face at later stages. In contrast, tadpoles with perturbed left (red) and right (blue) sides have branchial arch landmarks that are inappropriately close together and misplaced jaw landmarks at early stages. By late stages, the two halves of these faces are visibly more symmetrical and closely resemble the outlines of unaffected tadpoles.

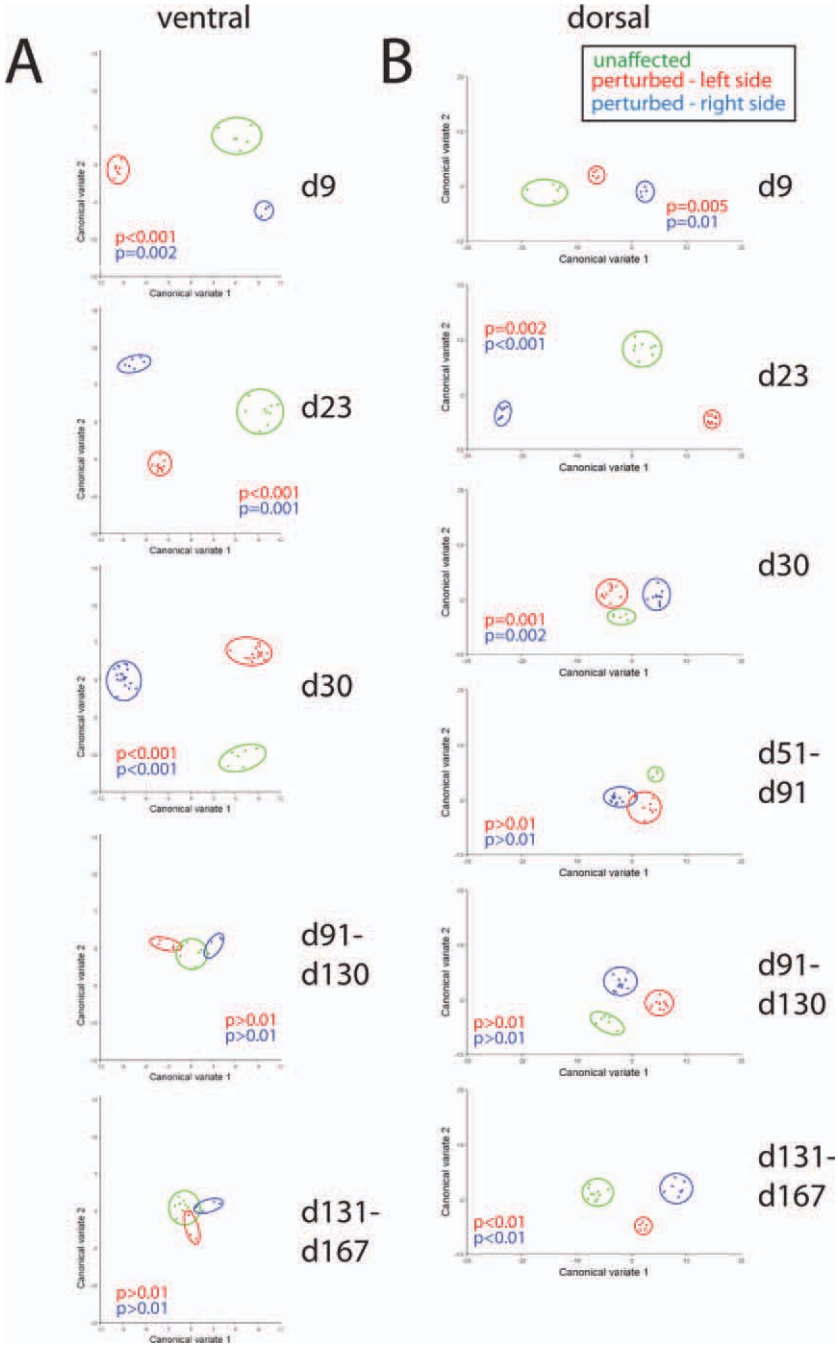

Fig. 5. Canonical variate analysis indicates that tadpoles with perturbed craniofacial features become indistinguishable from unaffected tadpoles. **A**: Analysis of ventral landmarks reveals significant differences between the three groups (unaffected [n = 10], perturbed left side [n = 17], perturbed right side [n = 19]) at early ages (d9, d23, d30). However, in later stages, these groups are no longer statistically distinguishable ($P > 0.01$). **B**: Canonical variate analysis reveals more complicated statistical relationships for dorsal landmarks. At early stages (d9, d23, d30) the three treatment groups are clearly different from each other. However, at d51–90 and d91–131, there are no longer any statistical differences distinguishing the perturbed groups from the unaffected controls ($P > 0.01$). Finally, at d131–167, both groups with perturbed faces were statistically distinguishable from unaffected controls ($P < 0.01$). For all panels, *P* values indicated in red are the differences between animals with perturbed left sides and unaffected controls. *P* values indicated in blue are the differences between animals with perturbed right sides and unaffected controls.

from correctly placed contralateral structures. Yet tadpoles with perturbations on both sides of the face (e.g., Fig. 1) also displayed a more normalized appearance over time, similar to those with unilateral perturbations. This suggests that a correct anatomical "template" for placement of craniofacial structures is not needed to direct the corrective movements and morphogenesis of affected craniofacial structures.

To further address whether craniofacial structures follow a predetermined program of morphological changes and movements, we calculated the relative differences in position of craniofacial landmarks between the youngest and oldest ages examined (Fig. 6A). We selected the anterior-most structures of the face, the jaw and nostrils, because they represent a CNC-derived feature (the jaw) and a placode-derived feature (the nose). For these analyses, the location of the left and right jaws and nostrils were mapped relative to the anterior-most point of the brain. The relative movements of these structures in the anterior–posterior and left–right axes were then calculated between the earliest (d9) and the latest (d167) ages examined (Fig. 6B).

In unaffected tadpoles, both the left and right jaws and nostrils moved in the anterior direction, relative to the brain, as the tadpoles aged (Fig. 6C); the total distance moved by the nostrils was greater than the distance moved by the jaws—the displacement of these structures relative to one another is not constant. Lateral movements (to the left and right sides of the face) were relatively minimal for all four facial structures examined. In tadpoles with perturbations on the left side, at early ages, the left jaw was closer to the front of the brain compared with the right jaw (Fig. 6A). However, by the last age examined, the left and right jaws were aligned appropriately. When quantified, the left jaw moved in the anterior direction significantly more than the movement of the same structure in unaffected controls; movement along the left–right axis, however, was minimal (Fig. 6C). Similarly, tadpoles with perturbed right sides had right jaws that were closer to the front of the brain than their counterparts on

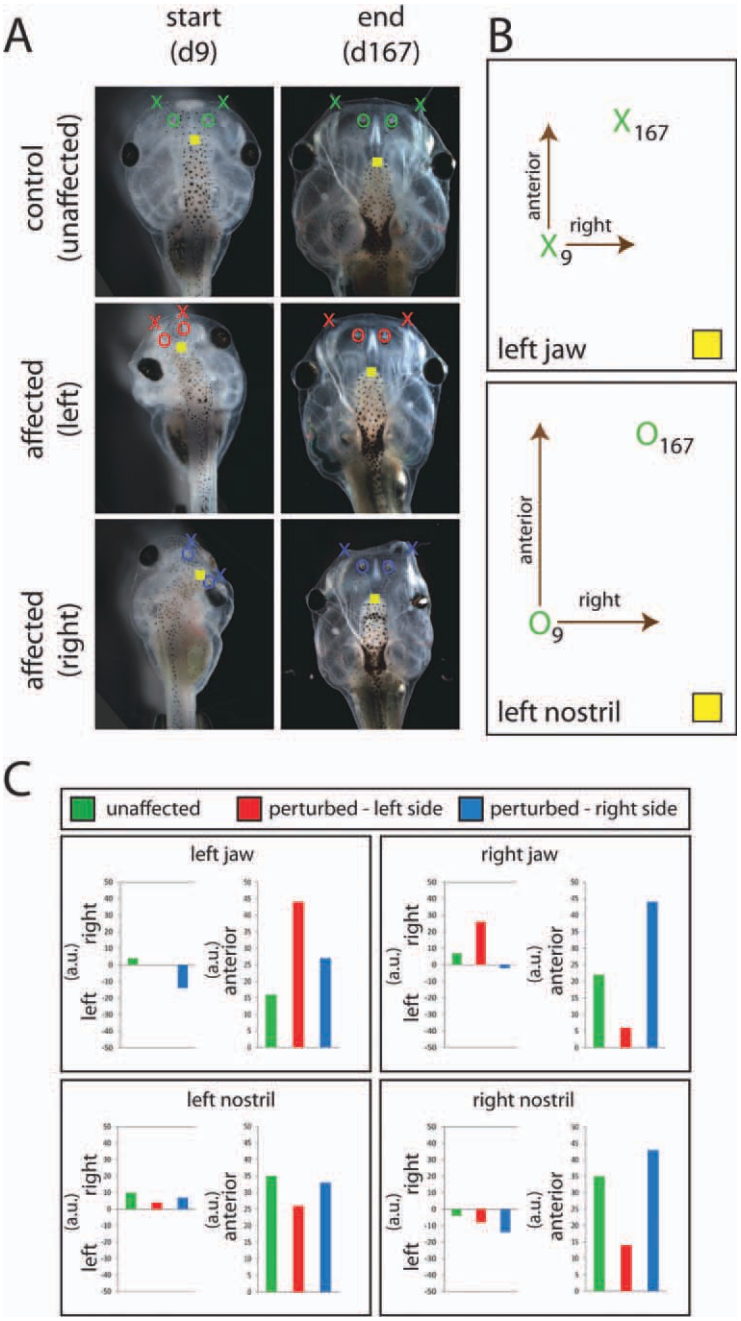

Fig. 6. Anterior structures "calculate" their distances from each other during the normalization process. **A**: Landmarks for the left and right jaws, and the left and right nostrils were located in images collected from all three groups at d9, d23, d30, d51–d90, d91–d130, and d131–d167. This image shows the location of jaws (X) and nostrils (O) in unaffected and perturbed tadpoles at the earliest and latest ages examined. **B**: To calculate the relative differences in location of each landmark along the anterior–posterior and left–right axes, the coordinates describing the position of each landmark at day 167 were subtracted from the coordinates describing the location of the same landmark at d9. Shown here are two examples of the relative differences in location of the left jaw and left nostril in unaffected tadpoles. Clearly, between d9 and d167, the left nostril moves further in the anterior and right directions compared with the jaw on the same side. **C**: Quantification of movements in the anterior–posterior and left–right axes for left and right jaws and nostrils. In unaffected tadpoles (green), the majority of movements between d9 and d131–167 were in the anterior direction with little movement along the left–right axis. Animals with perturbations on the left side (red) had extensive anterior movements of the left jaw that were more than twice the distance moved in unaffected tadpoles, and decreased movements in the anterior direction for structures on the right side (jaw and nostril). Animals with perturbations on the right side (blue) had heightened movements of the right jaw that were largely in the anterior direction. Sample sizes for all analyses: unaffected n = 10, perturbed left side n = 10, perturbed right side n = 9.

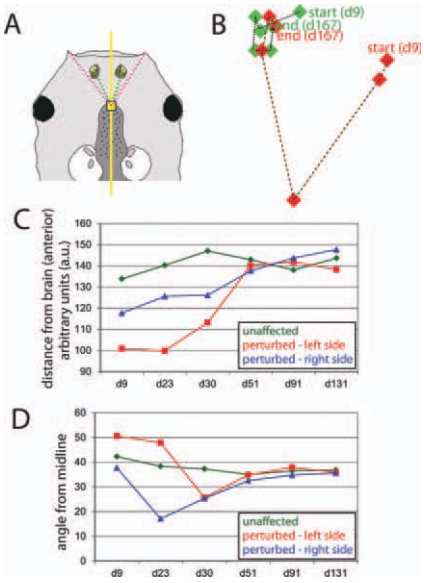

Fig. 7. Correct placement of craniofacial structures defined relative to the distance from the brain and the angle from the midline. **A**: Distances from the front of the brain (yellow square) were measured for nostrils (green dotted lines) and jaws (pink dotted lines) at each age. The angle from the midline (yellow line) was also calculated. **B**: As an example, the location of the left jaw is shown here at each timepoint measured for unaffected tadpoles (green) and tadpoles with perturbed left sides (red). The movements of the jaw in controls are relative minimal. In contrast, the position of the jaw is highly variable in animals with perturbed left sides. However, the final position of the jaw is very similar between these two groups. The movements of the jaw in controls are relative minimal. In contrast, the position of the jaw is highly variable in animals with perturbed left sides. However, the final position of the jaw is very similar between these two groups. **C**, **D**: When the distance from the brain and angle from the midline are quantified, it is clear that animals with perturbations in their craniofacial structures (red, perturbed left sides, n = 10; blue, perturbed right sides, n = 9) eventually achieve normal values for these parameters similar to those observed in unaffected controls (green, n = 10).

the left side (Fig. 6A). At the oldest age examined, symmetry had become restored between the distances from the front of the brain on the perturbed right side and unaffected left side. The right jaw moved in the anterior direction significantly more than the movement of the same structure in unaffected controls; movement along the left–right axis, however, was relatively minimal (Fig. 6C). We conclude that the jaw can determine its position relative to other craniofacial structures, and it uses this information to guide corrective movements

that ultimately produce a final morphology similar to that of an unaffected tadpole.

Distance From the Brain and Angle From the Midline Provide Normalization Parameters

How does each craniofacial structure determine whether it is in the correct place? We defined the anterior-most point of the brain as our reference location because it does not vary noticeably in affected tadpoles. We then measured the distance of each jaw and nostril from the anterior-most point of the brain (Figs. 6A, 7A), as well as the angle of the structure from the midline of the animal (Fig. 7A), at each age. We then calculated the distance and angle of these structures at each time point (Fig. 7B). In unaffected controls, there was some movement of structures relative to the brain and midline, but the calculated distance from the brain and the angle from the midline remained relatively constant over time (distance: 133–147 [arbitrary units, a.u.] from brain, angle: 35–42 degrees from the midline, Fig. 7C,D). In contrast, at the earliest ages examined, animals with perturbations on the left side had left jaws that were too close to the brain (distance: 99–101 a.u.) and at a more obtuse angle compared with controls (angle: 48–50 degrees from midline). Yet, over time, the distance and angle from the midline both came to resemble the measures of these features in unaffected controls. Similar results were observed for other anterior structures of the face (data not shown). These results suggest that the craniofacial structures can determine their relative position by a mechanism that can be modeled as detecting the distance and angle from the brain. Minimizing the error of these two parameters enables the structure to move until it reaches the appropriate position.

Normal Appearance of Most Craniofacial Structures Following Metamorphosis

The process of metamorphosis involves extensive remodeling of the craniofacial structures as the tadpole face undergoes the morphological changes necessary to produce froglet features (Trueb and Hanken, 1992; Slater et al., 2009). Does this remodeling proceed by means of a predetermined series of deformations appropriate to change a normal tadpole face into a frog, or do the processes of metamorphosis include mechanisms that enable self-monitoring and adaptive responses to changing initial conditions? To determine whether perturbations observed in the craniofacial structures of affected tadpoles would be maintained in froglets, we examined the morphology of the face of perturbed and unaffected individuals following metamorphosis. Of the 12 unaffected tadpoles that became froglets, none had visible morphologies that deviated from the expected appearance (Fig. 8A). An additional seven froglets were examined following metamorphosis of tadpoles with perturbations in the eye. In these individuals, the eye morphology remained abnormal, and several frogs developed eye tissue that was not accessible to the exterior of the animal. Finally, seven tadpoles that had obvious defects in CNC-derived structures (i.e., the jaw and/or branchial arches) were raised to froglet stages. Only one of these froglets had an external appearance that deviated from normal; the affected froglet had a minor protrusion of the jaw (Fig. 8A).

In addition to the analysis of external morphology, we asked whether the internal morphologies of craniofacial structures were normal in froglets produced from tadpoles with perturbed craniofacial structures by examining the morphology of craniofacial bones using a high resolution micro-computed tomography (CT) scan (Vasquez et al., 2008). These scans revealed surprisingly few differences between the jaw structures of frogs from unaffected tadpoles, and those from tadpoles that had serious jaw malformations at early stages (Fig. 8B). Only one froglet was observed to have deviations from the normal jaw morphology, having shortened jaw bones and an absent portion of the parasphenoid (a skull bone that covers the brain). We conclude that the calcified craniofacial structures in froglets raised from tadpoles with craniofacial perturbations had become remodeled toward a normal appearance, or only slight deviations from normal.

To determine the effect of early life perturbations on the soft tissue morphology of froglets, we also analyzed images collected using high resolution micro CT scans following treatment with 1% osmium tetroxide to visualize soft tissues (Skipper, 2006). These images showed obvious malformations in the eye tissue of froglets raised from tadpoles with eye deformities (Fig. 8C). For quantitative comparisons of exterior dorsal landmarks on froglet faces, we separated the froglets into four groups (unaffected controls, previously perturbed jaws/branchial arches, perturbed left eye and perturbed right eye) and compared these groups statistically using CVA. This analysis revealed that the position of craniofacial landmarks was significantly different in froglets with perturbed left or right eyes compared with unaffected controls (Fig. 8D). Importantly, there were no significant differences between unaffected controls and froglets raised from tadpoles with defects in their jaws/branchial arches. Thus, we conclude that tadpoles with perturbations in their jaws and other mouth structures had normalized completely; in contrast, animals with perturbed eyes remained distinguishable from untreated controls. These results reveal a remarkable ability of metamorphosis to achieve the same target morphology while starting from very different anatomical states.

DISCUSSION

The specification and morphogenesis of craniofacial structures has been the subject of a tremendous amount of research, aimed toward understanding the underlying etiology of human craniofacial disorders (Gitton et al., 2010; Kouskoura et al., 2011). Despite increased molecular-genetic insight into the pathways necessary for proper pattern formation, differentiation, and cell fate determination (Nuckolls et al., 1999), little is known about the mechanisms controlling the remodeling of these tissues at later ages (Parsons et al., 2011). The

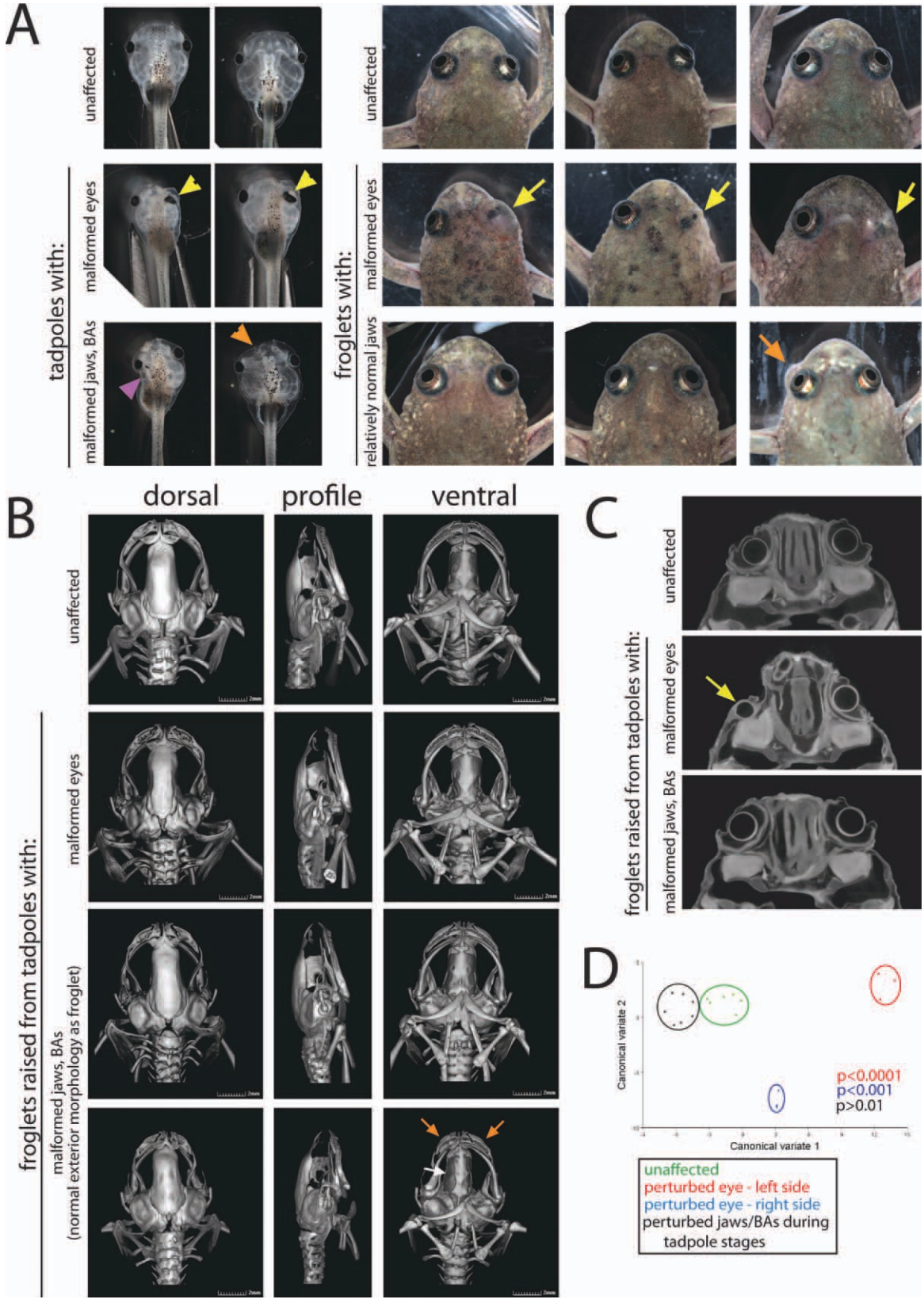

Fig. 8. Craniofacial structures following metamorphosis of unaffected and perturbed tadpoles. **A**: Froglets were raised from unaffected tadpoles or tadpoles with craniofacial perturbations. Tadpoles with eye malformations metamorphosed into frogs with severe eye deformities. In contrast, tadpoles with defects in their jaws and/or branchial arches developed into froglets with normal exterior morphologies. The one exception was a froglet with a slight protrusion of the skin under the left eye. **B**: High resolution CT scans reveal remarkably normal craniofacial bone structures in the faces of froglets raised from tadpoles with craniofacial malformations. One froglet had slightly narrowed jaw bones (orange arrows) and a small section of the parasphenoid bone was absent (white arrow). Three orientations are shown from each sample. **C**: High resolution CT images of soft tissues reveal eye deformities (yellow arrow) only in those froglets raised from tadpoles with eye malformations. These images show similar coronal planes through the heads of froglets. **D**: Canonical variate analysis indicates that animals with either left eye perturbations (red) or right eye perturbations (blue) are significantly different from unaffected controls (green). However, froglets that were raised from tadpoles with malformed jaws and/or branchial arches (black) were not distinguishable from unaffected controls. *P* values indicated in red are the differences between animals with perturbed left eyes and unaffected controls, *P* values indicated in blue are the differences between animals with perturbed right eyes and unaffected controls, and *P* values in black are the differences between animals with jaw/branchial arch defects during tadpole stages and unaffected controls.

proteins and enzymes involved in bone and cartilage remodeling are beginning to be understood in animal models of induced injury (Zambuzzi et al., 2009). Bone tissue in particular is a dynamic tissue, undergoing a constant cycle of resorption, reversal and formation throughout the life of an adult individual (Proff and Romer, 2009). Yet these processes have not been fully investigated in model organisms, and the ability to understand and manipulate them has obvious implications for restorative dentistry and the treatment of birth defects and facial injuries. Even less is known about the adaptive, dynamically regulated aspects of the mechanisms that may underlie robustness to perturbations of morphogenetic control networks. This is crucial, because such perturbations can occur not only as chance events from environmental insult, but also as the results of evolutionary change. Knowing how later stages are or are not affected by alterations in morphology at earlier stages is key to understanding modularity and evolvability of living forms.

Here, we used perturbation of endogenous bioelectrical mechanisms of craniofacial patterning to induce defects; future studies will extend this analysis to defects arising from the modulation of other pathways. We have shown that in the *Xenopus* tadpole, induced craniofacial malformations are intrinsically corrected as the animal ages (Figs. 1, 5). Specifically, tadpoles with malformed jaws and branchial arches that had obvious deformities 9 days after fertilization are largely indistinguishable from controls approximately 40–80 days later. In contrast, the eyes can achieve a more normal *location* over time, but typically maintain an abnormal *morphology*. Finally, the olfactory bulbs (nostrils) appear to move to the appropriate location, and also have a more normalized appearance over time, but a *completely normal* morphology is typically not achieved. These results suggest that some tissues may be more easily adaptable and repaired with time, whereas others can be somewhat repaired but never restored to a completely normal appearance. One plausible explanation for the differing ability of tissues to achieve a normal morphology is their embryonic origin. For example, we observe that tissues derived from CNC (jaw and branchial arch) are repositioned and remodeled to a high degree so that they reach the appropriate goal shape, but tissues derived from ectodermal placodes (eye and nose) are less capable of these feats. This could potentially be due to the more active, dynamic nature of CNC cells, which are known to implement path-finding during normal development. Another, nonmutually exclusive possibility is that the cells that contribute to placodes are terminally differentiated, but neural crest cells with pluriopotent properties may be retained in adulthood (Leucht et al., 2008; Cordero et al., 2010). Future studies are needed to address these hypotheses.

How does a structure determine where it is supposed to go within a deformed craniofacial landscape, i.e. one that it could not have been preprogrammed to navigate? The ability of tissues and organ primordia to achieve the appropriate target position and/or morphology and stop changing once this is achieved, despite abnormal starting states, could be interpreted as an ability to perform a kind of means-ends analysis. For example, the right jaw moves significantly in the anterior direction and slightly to the right, between the period of d9 to d167 (Fig. 6C). We have shown that this is not a set "program" of movements with predefined magnitude and direction, because animals with malformed right sides have jaws that move more than twice as far as unaffected controls in the anterior direction, and slightly to the left. Rather, our results are consistent with an information exchange process in which a structure triangulates its distance and angle from a stable reference point (e.g., the anterior of the brain and the angle from the midline), to achieve a normal position over time. Rather than simply moving to the correct distance and angle, each structure seems to wander until it reaches the appropriate point (e.g., the angle of the left jaw over time in animals with perturbations on the left side in Fig. 7D). The progression toward this correct state is not necessarily direct. For example, the jaw can "over-shoot" the correct angle at d30 before readjusting to an angle that more closely resembles the normal angle by d51.

These findings suggest an algorithmic, functional, and, importantly, testable model for how each craniofacial landmark is normalized to the correct position (Fig. 9). We propose that "pings" (information-containing signals) are exchanged between an 'organizing center' and each craniofacial structure. The "organizing center" responds with a "stop" message if the ping is both sent and returned in an appropriate manner; however, if the ping does not return, or possibly, if it has inappropriate speed, duration, amplitude, and/or frequency, no "stop" signal is sent, and the organ continues to migrate. One possible 'organizing center' is the brain and the well-developed neural network that innervates each sensory organ. Prior data may support this model: the frontonasal ectoderm and forebrain have been proposed to have organizing activity for embryonic craniofacial structures (Marcucio et al., 2005; Hu and Marcucio, 2009b), and during the stages when the facial structures are specified, the forebrain establishes gradients of sonic hedgehog protein, a morphogen that influences craniofacial morphogenesis (Hu and Marcucio, 2009a; Young et al., 2010). The eye has also been proposed to have organizing activity (Kish et al., 2011), as it generates gradients of retinoic acid (Rossant et al., 1991; Molotkov et al., 2006) which is also known to influence the patterning of craniofacial structures (Matt et al., 2005, 2008).

At this time, the molecular nature of the "ping" and "stop" signals are unknown, but future studies will shed light on the role of neural innervations and these morphogens in the normalization process, and suppression screens using pharmacological or genetic reagents to target specific communication pathways during this process will identify the mechanisms involved (Adams and Levin, 2006a,b). That the jaw "over-shoots" its correct position (Fig. 7D) sets lower limits on the timing of the mechanism controlling the sequence of ping/stop signals. If these signals were cycling very quickly, organ placement would not

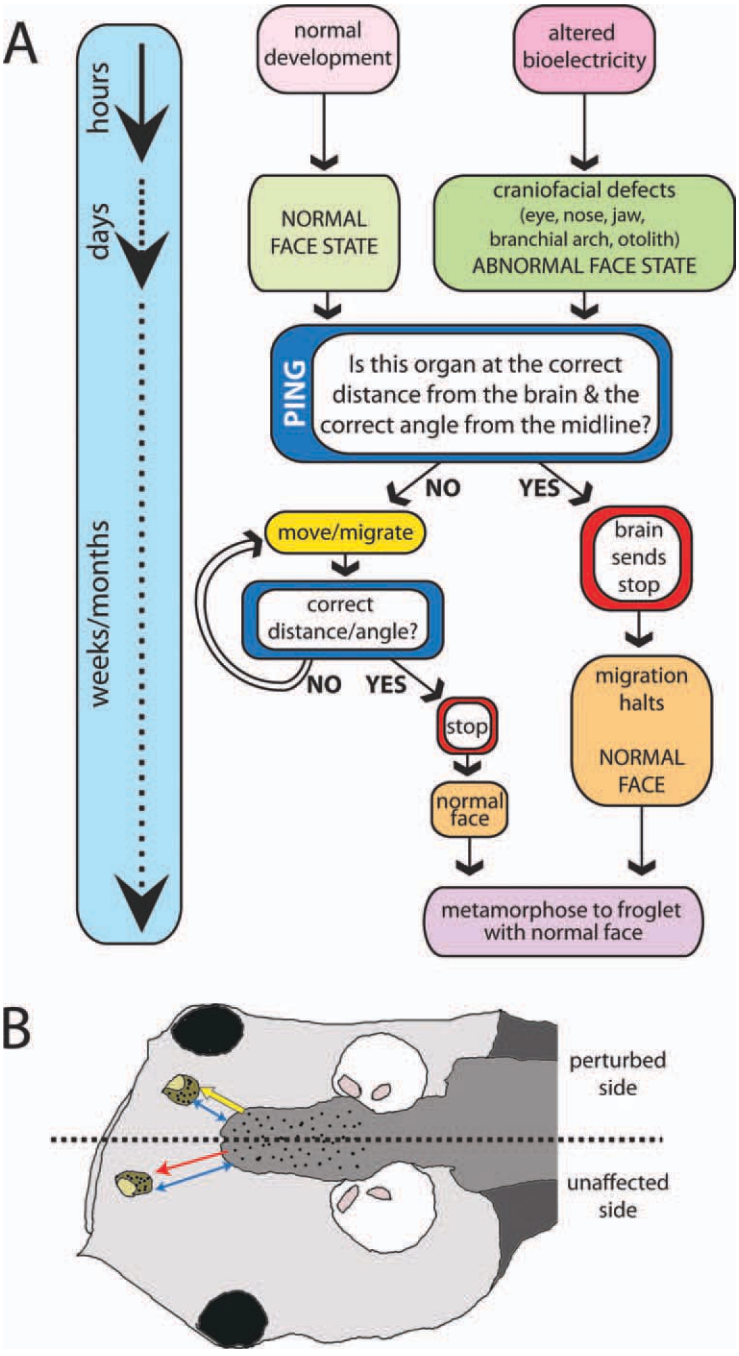

Fig. 9. An algorithmic model for the mechanism dictating normalized position of craniofacial structures. **A**: During the first few hours of life, perturbations in bioelectricity can produce abnormal face states that manifest within a few days of development. Over a period of several weeks/months, a "ping" signal is sent between an "organizing center" and each craniofacial structure. If the organ is positioned properly, the 'organizing center' communicates a "stop" signal, migration of the organ halts, and the resulting face is normal in both tadpole and froglet stages. If the organ is not positioned appropriately, no "stop" signal is given, so the organ moves/migrates and the cycle of "ping" and "move/migrate" continues until the organ is properly localized. **B**: This system of ping/move/stop occurs independently in each organ/structure. Thus, if for example the 'organizing center' is located in the forebrain, a ping (blue arrow) is communicated between the brain and each structure (for example, each nostril). If the location of a structure is correct (i.e. on the unaffected side of an individual), the "stop" signal is sent (red arrow). But if this stop signal is not sent, the organ continues to move (shown here as a mislocalized nostril on the perturbed side, yellow arrow).

require an over-correction because it would receive a "stop" signal as soon as it reached the correct distance and angle. Instead, each cycle of ping/stop is likely to encompass several weeks, in the case of *Xenopus*, requiring course correction over a longer period of time.

Finally, an interesting and surprising finding was revealed by the analysis of tadpoles with perturbed craniofacial structures: there are significant differences in the effects of abnormalities on the left and right sides of the face. When perturbations were targeted to only one side of the face, the uninjected side was often affected, but in a subtler manner compared with the injected side. For an example of this phenomenon, see the outlines in Figure 4A,B, which depict the deviations in landmark location in animals with perturbations on the left and right sides; the uninjected sides were clearly not normal at early ages. This may be due to physical forces "pulling" on the uninjected side, or could be due to effects earlier in development on predifferentiated mesoderm and ectoderm. A similar phenomenon has been described in human patients with asymmetric synostosis, where the facial features in the middle and lower face rotate toward the unaffected side (Oh et al., 2008), which requires surgical intervention to be corrected. Nevertheless, *consistently biased* differences in repair behavior suggests a link to the pathways that pattern the left–right axis of the body (Vandenberg and Levin, 2009, 2010).

We noted that perturbations affecting the left side often appear worse compared with those affecting the right side, and these sides appear to repair deformities in somewhat different ways (Figs. 6C, 7, data not shown). Thus, even though the facial structures are typically thought to be bilaterally symmetrical, there are underlying asymmetries that are more easily detected when defects are induced, as has been shown in planarian and zebrafish models (Albertson and Yelick, 2005; Nogi et al., 2005). This is not only relevant for basic studies of left–right patterning (Vandenberg and Levin, 2009), usually focused on asymmetric

viscera and brain, but also may have important implications for human health. Unilateral craniofacial deformities like cleft lip and cleft palate have a left–right bias, with significantly more of these birth defects occurring on the left side (Chenevix-Trench et al., 1992; Holder et al., 1992). Additionally, right-handed individuals use their right ear dominantly, and have larger structures on the left side of the face; these patterns are reversed in left-handed individuals (Dane et al., 2002, 2004). These results, together with our data, support the hypothesis that tissues and organs, including craniofacial structures, possess left–right positional information as well as the capacity to maintain left–right identities long after embryogenesis (Levin, 2005).

Studies are underway to identify which cellular processes are responsible for the observed changes in organ shape and position. Cell proliferation, apoptosis, altered mechanical properties (e.g. tissue density, turgidity of cells, tension in extracellular matrix molecules, etc.), specification and differentiation of cell types, and pattern formation all play important roles in dictating morphogenesis of embryonic structures (Pilot and Lecuit, 2005; Lecuit and Le Goff, 2007; Borghi and James Nelson, 2009; Martin, 2010), and regenerative states sometimes recapitulate early development (Martin and Parkhurst, 2004; Levin, 2007). Any of these processes could be involved in the normalization of perturbed faces. Additionally, future experiments will elucidate whether the effects we have observed are cell- or tissue-autonomous by grafting tissues from affected individuals into unaffected tissue environments and vice versa. Such grafting experiments will also reveal whether tissues derived from different embryonic precursors (i.e., neural crest cells versus placodes) are differently influenced by surrounding tissues.

Conceptually, normalization requires mechanisms that can determine whether or not a goal state has been reached by the morphogenesis system as a whole; this is important both for initiating compensatory change and for stopping rearrangements at the appropriate time. Numerous examples of shape self-monitoring exist in nature, including: the normal development of embryos split or joined at early stages, the correct orientation and size of regenerated limbs, hearts, and entire heads (Goss, 1969; Birnbaum and Alvarado, 2008), allometric scaling during whole-body remodeling in planaria (Oviedo et al., 2003), and the eventual transformation of a tail into a limb after a tail blastema is grafted at the flank in amphibia (Butler and O'Brien, 1942). In this last case, the ectopic tail slowly transforms into a limb—the structure appropriate to the new anatomical context into which the blastema is placed (Guyenot, 1927; Guyenot and Schotte, 1927; Farinella-Ferruzza, 1953, 1956). Information about position within the body is essential for remodeling, and indeed, many models in developmental and regenerative biology make use of the concept of positional information (French et al., 1976; Shi and Borgens, 1995; Niehrs, 2010; Ogawa and Miyake, 2011), which appears to be maintained throughout adulthood (Chang et al., 2002; Wang et al., 2009). Morphometric analyses will help determine which quantities might be measured, conserved, or optimized during these or other examples of regulated morphogenesis. These will generate more testable mechanistic models. A more difficult challenge is the dissection of mechanisms that induce coherent cell groups to perform behaviors appropriate to eventually reach the goal state.

Although there are a wide range of diverse craniofacial morphologies throughout vertebrate animals, and some divergence for the mechanisms used to build craniofacial structures during embryogenesis, there is remarkable conservation in the molecular mechanisms dictating neural crest induction, specification, migration and differentiation (Minoux and Rijli, 2010). Thus, our findings may have wider implications, including the possibility that human craniofacial structures can be induced to self-repair. In fact, throughout adulthood, the human face does remodel, with significant and consistent changes observed in skeletal and soft tissues (Sharabi et al., 2010). Therefore, the prospect of harnessing the craniofacial tissues' inherent abilities to remodel may not be far-fetched, and less-invasive techniques for repairing human birth defects may be possible. More broadly, understanding the ontogeny and evolution of morphogenesis involves fleshing out the mechanisms that link the genetic code to topological outcomes. The remarkable robustness of endogenous patterning control systems suggests that what the genetic programs encode is not specific shapes or movements at specific times; rather, the interplay of gene regulatory networks and biophysical events implement highly robust, adaptive programs with information processing capabilities that enable a target morphology to be reached by different paths and stabilized as an optimized state. Uncovering the mechanisms by which structures ascertain their own position and orientation within the host is a key step toward predictive control of morphology for regenerative medicine applications, as well as for the bioengineering of living computational systems in synthetic biology.

EXPERIMENTAL PROCEDURES

Generation of Craniofacial Phenotypes

All experiments were approved by the Tufts University Animal Research Committee in accordance with the Guide for Care and Use of Laboratory Animals. *Xenopus* embryos were collected according to standard protocols (Sive et al., 2000). At the appropriate stage, embryos were placed in Ficoll and injected with capped, synthetic mRNAs; rhodamine-labeled dextran or Alexa647-labeled dextran was used as a lineage tracer. For all injections, a truncated ductin mutant (*xduct-no TM4*) was injected into one-cell or two-cell embryos (Vandenberg et al., 2011); this protein lacks the proton binding site entirely (Nishi and Forgac, 2002), thus it alters both pH and membrane voltage, two factors that influence craniofacial morphogenesis (Vandenberg et al., 2011).

After injection, embryos were washed and placed in 0.1× Modified Marc's Ringers (MMR) pH 7.8. At Nieuwkoop

and Faber stage 45–46, when phenotypes became clearly visible, control and treated tadpoles were anesthetized with 1.5% MS-222 (tricaine) and then scored for craniofacial phenotypes. The tricaine was washed out and tadpoles were housed in groups according to the type of perturbation observed. The most severely affected individuals were not used in these experiments due to failure to thrive. However, all tadpoles included in the analysis had clearly visible perturbations in one or more craniofacial structure.

Maintenance and Imaging of Developing Tadpoles

After tadpoles were separated into groups by type of craniofacial perturbation, they were maintained in 0.1× MMR at 14–18°C. Controls consisted of injected unaffected tadpoles and untreated tadpoles; these were cared for in the same way as the groups with craniofacial perturbations. All tadpoles were fed 4–5 times per week a diet of spirulina and finely ground frog brittle and were cleaned within 8 hr of feeding. At several intervals, tadpoles were anesthetized with tricaine and imaged using a Nikon SMZ1500 dissection microscope with a Retiga 2000R camera and ImageQ software. Following imaging, they were returned to their cages and fed. Photoshop was used to orient, scale, and improve clarity of images. Data were neither added nor subtracted; original images are available on request. Tadpoles were no longer imaged when they reached stages 55–57 and were allowed to metamorphose naturally.

Froglet Care and Euthanasia

Froglets were housed for approximately 1–2 months after the completion of metamorphosis. During that time, they were fed three to five times per week and cleaned within 8 hr of feeding. Froglets were killed by an overdose of benzocaine and a cut was made through the stomach cavity to ensure penetrance of fixative. Killed froglets were fixed in 10% neutral buffered formalin (NBF) and maintained in 10% NBF for bone and soft tissue analysis.

Morphometric Analysis of Tadpole and Froglet Craniofacial Structures

Images collected at various ages of tadpole development were analyzed for the position of landmarks with ImageJ software (version 1.44; NIH). For dorsal images, a total of 12 landmarks were determined: (1) right nostril; (2) right barbel/outer edge of mouth; (3) inner point of right eye; (4) outer point of right eye; (5) right otocyst; (6) left otocyst; (7) inner point of left eye; (8) outer point of left eye; (9) left barbel/outer edge of mouth; (10) left nostril; (11) midpoint of the front of the brain; (12) midpoint of brain between otocysts.

For ventral images, a total of 20 landmarks were determined: (1) upper inner edge of left branchial arch; (2) inner edge of left 2nd gill arch; (3) inner edge of left 3rd gill arch; (4) inner edge of right 3rd gill arch; (5) inner edge of right 2nd gill arch; (6) upper inner edge of right branchial arch; (7) outer edge of left 2nd gill arch; (8) outer edge of left 3rd gill arch; (9) bottom outer edge of left branchial arch; (10) bottom outer edge of right branchial arch; (11) outer edge of right 3rd gill arch; (12) outer edge of right 2nd gill arch; (13) inner point of right eye; (14) outer point of right eye; (15) right lower jaw/barbel; (16) left lower jaw/barbel; (17) outer point of left eye; (18) inner point of left eye; (19) midpoint of front of jaw; (20) midpoint between the top of the left and right branchial arches. See Figure 3 for illustration of these points and examples from unaffected and unilaterally perturbed tadpoles.

For morphometric analyses of froglets, a total of 8 landmarks were selected: (1) right nostril; (2) left nostril; (3) outer point of left eye; (4) inner point of left eye; (5) inner point of right eye; (6) outer point of right eye; (7) front edge of parasphenoid bone; (8) midpoint of front of jaw.

Once X,Y coordinates were collected for each landmark using ImageJ, morphometric analyses were performed with MorphoJ software (Klingenberg, 2011). First, data for dorsal and ventral analyses were aligned using Procrustes superimposition (using landmarks 11 and 12 for dorsal images, landmarks 19 and 20 for ventral images or landmarks 7 and 8 for froglet images) and a covariance matrix was produced. To examine the shapes of dorsal and ventral structures in unaffected and affected tadpoles, principle components analysis was used to generate a description of the variance in shape of the tadpoles within each treatment and age group. To facilitate visualization, separate outlines, based on average landmark positions, were generated for animals with affected left and right sides. To statistically compare the three groups (unaffected, perturbed left side and perturbed right side) at each age, canonical variate analysis was performed on dorsal and ventral landmarks. For canonical variate analysis of froglets, four groups were compared (froglets derived from tadpoles with unaffected faces, left eye perturbations, right eye perturbations, or perturbations of the jaw and/or branchial arch.) Groups were considered statistically distinguishable at $P < 0.01$.

Micro-CT Scan of Froglets

Intact whole-animal CT scans were performed (Numira Biosciences, Salt Lake City UT) on fixed froglets and volume rendering was used to create images of the craniofacial skeletal structures. For soft tissue scans, fixed froglets were treated with 1% osmium tetroxide and whole animal CT scans were then performed.

ACKNOWLEDGMENTS

The authors thank Punita Koustubhan, Amber Currier, Claire Stevenson, Brian Pennarola, and Ryan Morrie for *Xenopus* husbandry and tadpole care, and members of the Levin lab for helpful discussions. L.N.V. was funded by the NRSA, D.S.A. was funded by a NIH grant, and M.L. was funded by a grant from the G. Harold and Leila Y. Mathers Charitable Foundation.

REFERENCES

Adams DS, Levin M. 2006a. Inverse drug screens: a rapid and inexpensive method for implicating molecular targets. Genesis 44:530–540.

Adams DS, Levin M. 2006b. Strategies and techniques for investigation of biophysical signals in patterning. In: Whitman M, Sater AK, editors. Analysis of growth factor signaling in embryos. Philadelphia: Taylor and Francis Books. p 177–262.

Albertson RC, Yelick PC. 2005. Roles for fgf8 signaling in left-right patterning of the visceral organs and craniofacial skeleton. Dev Biol 283:310–321.
Alfandari D, Cousin H, Marsden M. 2010. Mechanism of Xenopus cranial neural crest cell migration. Cell Adh Migr 4: 553–560.
Basch ML, Garcia-Castro MI, Bronner-Fraser M. 2004. Molecular mechanisms of neural crest induction. Birth Defects Res C Embryo Today 72:109–123.
Birnbaum KD, Alvarado AS. 2008. Slicing across kingdoms: regeneration in plants and animals. Cell 132:697–710.
Borghi N, James Nelson W. 2009. Intercellular adhesion in morphogenesis: molecular and biophysical considerations. Curr Top Dev Biol 89:1–32.
Brooks DR, Wiley EO. 1988. Evolution as entropy: toward a unified theory of biology. Chicago: University of Chicago Press. xiv, 415 pp.
Brugmann SA, Moody SA. 2005. Induction and specification of the vertebrate ectodermal placodes: precursors of the cranial sensory organs. Biol Cell 97:303–319.
Brugmann SA, Cordero DR, Helms JA. 2010. Craniofacial ciliopathies: a new classification for craniofacial disorders. Am J Med Genet A 152A:2995–3006.
Butler EG, O'Brien JP. 1942. Effects of localized X-irradiation on regeneration of the Urodele limb. Anat Rec 84:407–413.
Chang HY, Chi JT, Dudoit S, Bondre C, van de Rijn M, Botstein D, Brown PO. 2002. Diversity, topographic differentiation, and positional memory in human fibroblasts. Proc Natl Acad Sci U S A 99:12877–12882.
Chenevix-Trench G, Jones K, Green AC, Duffy DL, Martin NG. 1992. Cleft lip with or without cleft palate: associations with transforming growth factor alpha and retinoic acid receptor loci. Am J Hum Genet 51:1377–1385.
Cooper WJ, Parsons K, McIntyre A, Kern B, McGee-Moore A, Albertson RC. 2010. Bentho-pelagic divergence of cichlid feeding architecture was prodigious and consistent during multiple adaptive radiations within African rift-lakes. PLoS One 5:e9551.
Cordero DR, Brugmann S, Chu Y, Bajpal R, Jame M, Helms JA. 2010. Cranial neural crest cells on the move: their roles in craniofacial development. Am J Med Genet A 155:270–279.
Couzin ID. 2009. Collective cognition in animal groups. Trends Cogn Sci 13:36–43.
Dane S, Gumustekin K, Polat P, Uslu C, Akar S, Dastan A. 2002. Relations among hand preference, craniofacial asymmetry, and ear advantage in young subjects. Percept Mot Skills 95: 416–422.
Dane S, Ersoz M, Gumustekin K, Polat P, Dastan A. 2004. Handedness differences in widths of right and left craniofacial regions in healthy young adults. Percept Mot Skills 98:1261–1264.
Deisboeck TS, Couzin ID. 2009. Collective behavior in cancer cell populations. Bioessays 31:190–197.
Dolk H, Loane M, Garne E. 2010. The prevalence of congenital anomalies in Europe. Adv Exp Med Biol 686: 349–364.
Farinella-Ferruzza N. 1953. Risultati di trapianti di bottone codale di urodeli su anuri e vice versa. Riv Biol 45:523–527.
Farinella-Ferruzza N. 1956. The transformation of a tail into a limb after xenoplastic transformation. Experientia 15: 304–305.
French V, Bryant PJ, Bryant SV. 1976. Pattern regulation in epimorphic fields. Science 193:969–981.
Frieden BR. 1998. Physics from Fisher information: a unification. Cambridge, UK: Cambridge University Press. ix, 318 p.
Gitton Y, Heude E, Vieux-Rochas M, Benouaiche L, Fontaine A, Sato T, Kurihara Y, Kurihara H, Couly G, Levi G. 2010. Evolving maps in craniofacial development. Semin Cell Dev Biol 21: 301–308.
Goodwin BC. 1964. A statistical mechanics of temporal organization in cells. Symp Soc Exp Biol 18:301–326.
Goss RJ. 1969. Principles of regeneration. New York, NY: Academic Press. 287 p.
Guyenot E. 1927. Le probleme morphogenetique dans la regeneration des urodeles: determination et potentialites des regenerats. Rev Suisse Zool 34: 127–155.
Guyenot E, Schotte OE. 1927. Greffe de regenerat et differenciation induite. Comptes Rendus de Societe de Phys His Nat Geneve 44:21–23.
Harris SM, Ross AH. 2008. Detecting an undiagnosed case of nonsyndromic facial dysmorphism using geometric morphometrics. J Forensic Sci 53:1308–1312.
Hart TC, Hart PS. 2009. Genetic studies of craniofacial anomalies: clinical implications and applications. Orthod Carniofac Res 12:212–220.
Holder SE, Vintiner GM, Farren B, Malcolm S, Winter RM. 1992. Confirmation of an association between RFLPs at the transforming growth factor-alpha locus and non-syndromic cleft lip and palate. J Med Genet 29:390–392.
Hu D, Marcucio RS. 2009a. A SHH-responsive signaling center in the forebrain regulates craniofacial morphogenesis via the facial ectoderm. Development 136:107–116.
Hu D, Marcucio RS. 2009b. Unique organization of the frontonasal ectodermal zone in birds and mammals. Dev Biol 325:200–210.
Jones NC, Lynn ML, Gaudenz K, Sakai D, Aoto K, Rey J-P, Glynn EF, Ellington L, Du C, Dixon J, Dixon MJ, Trainor PA. 2008. Prevention of the neurocristopathy Treacher Collins syndrome through inhibition of p53 function. Nat Med 14:125–133.
Kendall DG. 1977. The diffusion of shape. Adv Appl Probability 9:428–430.
Kish PE, Bohnsack BL, Gallina D, Kasprick DS, Kahana A. 2011. The eye as an organizer of craniofacial development. Genesis 49:222–230.
Klingenberg CP. 2011. MorphoJ: an integrated software package for geometric morphometrics. Mol Ecol Resour 11: 353–357.
Klingenberg CP, Wetherill L, Rogers J, Moore E, Ward R, Autti-Ramo I, Fagerlund A, Jacobson SW, Robinson LK, Hoyme HE, Mattson SN, Li TK, Riley EP, Foroud T. 2010. Prenatal alcohol exposure alters the patterns of facial asymmetry. Alcohol 44:649–657.
Kouskoura T, Fragou N, Alexiou M, John N, Sommer L, Graf D, Katsaros C, Mitsiadis TA. 2011. The genetic basis of craniofacial and dental abnormalities. Schweiz Monatsschr Zahnmed 121: 636–646.
Langton CG. 1995. Artificial life: an overview. Cambridge, MA: MIT Press. xi, 340, [346] of plates pp.
Lecuit T, Le Goff L. 2007. Orchestrating size and shape during morphogenesis. Nature 450:189–192.
Leucht P, Kim JB, Amasha R, James AW, Girod S, Helms JA. 2008. Embryonic origin and Hox status determine progenitor cell fate during adult bone regeneration. Development 135:2845–2854.
Levin M. 2005. Left-right asymmetry in embryonic development: a comprehensive review. Mech Dev 122:3–25.
Levin M. 2007. Large-scale biophysics: ion flows and regeneration. Trends Cell Biol 17:262–271.
Marcucio RS, Cordero DR, Hu D, Helms JA. 2005. Molecular interactions coordinating the development of the forebrain and face. Dev Biol 284:48–61.
Martin AC. 2010. Pulsation and stabilization: contractile forces that underlie morphogenesis. Dev Biol 341:114–125.
Martin P, Parkhurst SM. 2004. Parallels between tissue repair and embryo morphogenesis. Development 131:3021–3034.
Matt N, Dupe V, Garnier JM, Dennefeld C, Chambon P, Mark M, Ghyselinck NB. 2005. Retinoic acid-dependent eye morphogenesis is orchestrated by neural crest cells. Development 132:4789–4800.
Matt N, Ghyselinck NB, Pellerin I, Dupe V. 2008. Impairing retinoic acid signalling in the neural crest cells is sufficient to alter entire eye morphogenesis. Dev Biol 320:140–148.
Mayor R, Aybar MJ. 2001. Induction and development of neural crest in Xenopus laevis. Cell Tissue Res 305:203–209.
Minoux M, Rijli FM. 2010. Molecular mechanisms of cranial neural crest cell migration and patterning in craniofacial development. Development 137: 2605–2621.
Molotkov A, Molotkova N, Duester G. 2006. Retinoic acid guides eye morphogenetic movements via paracrine signaling but is unnecessary for retinal dorsoventral patterning. Development 133:1901–1910.
Mondia JP, Levin M, Omenetto FG, Orendorff RD, Branch MR, Adams DS. 2011. Long-distance signals are required for morphogenesis of the regenerating Xenopus tadpole tail, as shown by femtosecond-laser ablation. PloS One 6:e24953.

Niehrs C. 2010. On growth and form: a Cartesian coordinate system of Wnt and BMP signaling specifies bilaterian body axes. Development 137:845–857.
Nishi T, Forgac M. 2002. The vacuolar (H+)-ATPases–nature's most versatile proton pumps. Nat Rev Mol Cell Biol 3: 94–103.
Nogi T, Yuan YE, Sorocco D, Perez-Tomas R, Levin M. 2005. Eye regeneration assay reveals an invariant functional left-right asymmetry in the early bilaterian, Dugesia japonica. Laterality 10:193–205.
Nuckolls GH, Shum L, Slavin HC. 1999. Progress toward understanding craniofacial malformations. Cleft Palate Craniofac J 36:12–26.
Ogawa K, Miyake Y. 2011. Generation model of positional values as cell operation during the development of multicellular organisms. Biosystems 103:400–409.
Oh AK, Wong J, Ohta E, Rogers GF, Deutsch CK, Mulliken JB. 2008. Facial asymmetry in unilateral coronal synostosis: long-term results after fronto-orbital advancement. Plast Reconstr Surg 121:545–562.
Oviedo NJ, Newmark PA, Sanchez Alvarado A. 2003. Allometric scaling and proportion regulation in the freshwater planarian Schmidtea mediterranea. Dev Dyn 226:326–333.
Parsons KJ, Andreeva V, Cooper WJ, Yelick PC, Albertson RC. 2011. Morphogenesis of the zebrafish jaw: development beyond the embryo. Methods Cell Biol 101:225–248.
Pilot F, Lecuit T. 2005. Compartmentalized morphogenesis in epithelia: from cell to tissue shape. Dev Dyn 232:685–694.
Proff P, Romer P. 2009. The molecular mechanism behind bone remodelling: a review. Clin Oral Invest 13:355–362.
Ross AH, Williams SE. 2010. Craniofacial growth, maturation, and change: teens to midadulthood. J Craniofac Surg 21: 458–461.
Rossant J, Zirngibl R, Cado D, Shago M, Giguere V. 1991. Expression of a retinoic acid response element-hsplacZ transgene defines specific domains of transcriptional activity during mouse embryogenesis. Genes Dev 5:1333–1344.
Saadeh PB, Chang CC, Warren SM, Reavey P, McCarthy JG, Siebert JW. 2008. Microsurgical correction of facial contour deformities in patients with craniofacial malformations: a 15-year experience. Plast Reconstr Surg 121: 368e–378e.
Sadaghiani B, Thiebaud CH. 1987. Neural crest development in the Xenopus laevis embryo, studied by interspecific transplantation and scanning electron microscopy. Dev Biol 124:91–110.
Sant'Anna LB, Tosello DO. 2006. Fetal alcohol syndrome and developing craniofacial and dental structures–a review. Orthod Carniofac Res 9:172–185.
Schlosser G. 2006. Induction and specification of cranial placodes. Dev Biol 294: 303–351.
Sharabi SE, Hatef DA, Koshy JC, Hollier LHJ, Yaremchuk MJ. 2010. Mechanotransduction: the missing link in the facial aging puzzle? Aesth Plast Surg 34: 603–611.
Shi R, Borgens RB. 1995. Three-dimensional gradients of voltage during development of the nervous system as invisible coordinates for the establishment of embryonic pattern. Dev Dyn 202:101–114.
Siegfried T. 2000. The bit and the pendulum: from quantum computing to M theory– the new physics of information. New York: Wiley. vi, 281 p.
Singh GD. 2008. Digital diagnostics: three-dimensional modelling. Br J Oral Maxillofac Surg 46:22–26.
Singh GD, Levy-Bercowski D, Santiago PE. 2005. Three-dimensional nasal changes following nasoalveolar molding in patients with unilateral cleft lip and palate: geometric morphometrics. Cleft Palate Craniofac J 42:403–409.
Sive H, Grainger RM, Harland R. 2000. Early development of Xenopus laevis. New York: Cold Spring Harbor Laboratory Press.
Skipper M. 2006. No Mickey-Mouse phenomics. Nat Rev Genet 7:409.
Slater BJ, Liu KJ, Kwan MD, Quarto N, Longaker MT. 2009. Cranial osteogenesis and suture morphology in Xenopus laevis: a unique model system for studying craniofacial development. PLoS One 4:e3914.
Streit A. 2007. The preplacodal region: an ectodermal domain with multipotential progenitors that contribute to sense organs and cranial sensory ganglia. Int J Dev Biol 51:447–461.
Suzuki D, Brandley MC, Tokita M. 2010. The mitochondrial phylogeny of an ancient lineage of ray-finned fishes (Polypteridae) with implications for the evolution of body elongation, pelvic fin loss, and craniofacial morphology in Osteichthyes. BMC Evol Biol 10:21.
Theveneau E, Mayor R. 2011. Collective cell migration of the cephalic neural crest: the art of integrating information. Genesis 49:164–176.
Trueb L, Hanken J. 1992. Skeletal development in Xenopus laevis (Anura: Pipidae). J Morphol 214:1–41.
Vandenberg LN, Levin M. 2009. Perspectives and open problems in the early phases of left-right patterning. Semin Cell Dev Biol 20:456–463.
Vandenberg LN, Levin M. 2010. Far from solved: a perspective on what we know about early mechanisms of left-right asymmetry. Dev Dyn 239:3131–3146.
Vandenberg LN, Morrie RD, Adams DS. 2011. V-ATPase-dependent ectodermal voltage and pH regionalization are required for craniofacial morphogenesis. Dev Dyn 240:1889–1904.
Vasquez SX, Hansen MS, Bahadur AN, Hockin MF, Kindlmann GL, Nevell L, Wu IQ, Grunwald DJ, Weinstein DM, Jones GM, Johnson CR, Vandeberg JL, Capecchi MR, Keller C. 2008. Optimization of volumetric computed tomography for skeletal analysis of model genetic organisms. Anat Rec (Hoboken) 291:475–487.
von Cramon-Taubadel N, Frazier BC, Lahr MM. 2007. The problem of assessing landmark error in geometric morphometrics: theory, methods, and modifications. Am J Phys Anthropol 134:24–35.
Voskoboynik A, Simon-Blecher N, Soen Y, Rinkevich B, De Tomaso AW, Ishizuka KJ, Weissman IL. 2007. Striving for normality: whole body regeneration through a series of abnormal generations. FASEB J 21:1335–1344.
Wang KC, Helms JA, Chang HY. 2009. Regeneration, repair and remembering identity: the three Rs of Hox gene expression. Trends Cell Biol 19:268–275.
Weber B, Depew D, Smith J. 1988. Entropy, information, and evolution. Cambridge, MA: MIT Press.
Weisensee KE, Jantz RL. 2011. Secular changes in craniofacial morphology of the portuguese using geometric morphometrics. Am J Phys Anthropol 145: 548–559.
Young NM, Chong HJ, Hu D, Hallgrimsson B, Marcucio RS. 2010. Quantitative analyses link modulation of sonic hedgehog signaling to continuous variation in facial growth and shape. Development 137:3405–3409.
Zambuzzi WF, Paiva KB, Menezes R, Oliveira RC, Taga R, Granjeiro JM. 2009. MMP-9 and CD68(+) cells are required for tissue remodeling in response to natural hydroxyapatite. J Mol Histol 40:301–309.